Recent studies of Charmonium Decays at CLEO

H. Muramatsu
Department of Physics and Astronomy, University of Rochester, Rochester, New York 14627, USA

Recent results on Charmonium decays are reviewed which includes two-, three- and four-body decays of χ_{cJ} states, observations of Y(4260) through $\pi\pi J/\psi$ transitions, precise measurements of $M(D^0)$, $M(\eta)$ as well as $\mathcal{B}(\eta \to X)$.

1. Introduction

Decays of a bound state of a quark and its anti-quark, quarkonium, provide an excellent laboratory for studying QCD. Particularly, heavy quarkonia such as charmonium states are less relativistic, thus play a special role in probing strong interactions.

CLEO recently has accumulated data taken at the $\psi(2S)$ resonance, providing a total of 27M $\psi(2S)$ decays. With the combination of this large statistical sample and the excellent CLEO detector, we will explore an unprecedented world of charmonia. While many analyses are currently being carried out, in this note we present recent results on multi-body χ_{cJ} decays which employed the pre-existing 3M $\psi(2S)$ sample.

We also present recent studies on decays of one of the exotic states, Y(4260), as well as precision measurement on $M(D^0)$ that has an implication on properties of X(3872).

Finally, based on the full sample of $\psi(2S)$ data, we have results on properties of one of the light mesons, η.

2. Factory of $\chi_c(1^3P_J)$ states

$\chi_c(1^3P_J)$ states, which have one unit of orbital angular momentum and total spin of J=0, 1, or 2, cannot be produced directly from e^+e^- collisions. They can be reached from $\psi(2S)$ through radiative (electric dipole) transitions. Since $\mathcal{B}(\psi(2S) \to \gamma\chi_{cJ}) = (9.3 \pm 0.4, 8.8 \pm 0.4, \text{and } 8.1 \pm 0.4) \times 10^{-2}$ for J=0, 1, and 2 respectively [1], 27M $\psi(2S)$ decays of the new data provides ∼2M decays of each spin state of χ_{cJ} which should give us a greater understanding of the decay mechanisms of the χ_{cJ} mesons.

In this section, we present recent results of studies of χ_{cJ} decays based on 3M $\psi(2S)$ decays which should serve as the foundation for the future precision measurements by employing the full data sample of 27M of $\psi(2S)$ decays.

2.1. Two-body decay

We present results on χ_{cJ} decay into combinations of η and η' mesons. Figure 1 shows invariant masses of combinations of η and η'. No χ_{c1} is seen as expected from conservation of spin-parity.

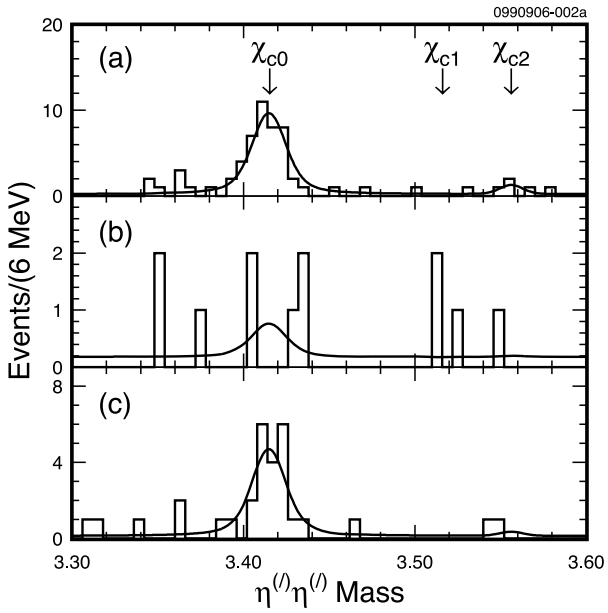

Figure 1: Invariant masses of $\eta\eta$ (a), $\eta'\eta$ (b), and $\eta'\eta'$ (c)

We measured $\mathcal{B}(\chi_{c0} \to \eta\eta)$ to be $(0.31 \pm 0.05 \pm 0.04 \pm 0.02)\%$ [2] where the first uncertainty is statistical, the second is systematic, and the third is systematic due to the uncertainty in $\mathcal{B}(\psi(2S) \to \gamma\chi_{cJ})$. This is slightly higher, but consistent with, the two previously published measurements. The BES Collaboration measured this branching ratio to be $(0.194 \pm 0.085 \pm 0.059)\%$ [3] and the E-835 Collaboration [4] had $(0.198 \pm 0.068 \pm 0.037)\%$. We also measured $\mathcal{B}(\chi_{c0} \to \eta'\eta')$ to be $(0.17 \pm 0.04 \pm 0.02 \pm 0.01)\%$ for the first time. We set upper limits for $\mathcal{B}(\chi_{c0} \to \eta\eta') < 0.05\%$, $\mathcal{B}(\chi_{c2} \to \eta\eta) < 0.047\%$, $\mathcal{B}(\chi_{c2} \to \eta\eta') < 0.023\%$, and $\mathcal{B}(\chi_{c2} \to \eta'\eta') < 0.031\%$ at 90% confidence level.

Our result can be compared to predictions based on the model of Qiang Zhao [5]. He translates these decay rates into a QCD parameter, r, which is the ratio of doubly- to singly-OZI suppressed decay diagrams. In his model, our results indicate that the singly-OZI suppressed diagram dominates in these decays.

2.2. Three-body decay

We have also looked at three-body decays of χ_{cJ} states (one neutral and 2 charged hadrons) [6]. They are $\pi^+\pi^-\eta$, $K^+K^-\eta$, $p\bar{p}\eta$, $\pi^+\pi^-\eta'$, $K^+K^-\pi^0$, $p\bar{p}\pi^0$, $\pi^+K^-K^0_S$, and $K^+\bar{p}\Lambda$. Measured branching fractions are summarized in Table I. Again, our results are consistent with the results from BES Collaboration [7], with better precision.

In three of the above modes we looked for, $\pi^+\pi^-\eta$, $K^+K^-\pi^0$, and $\pi^+K^-K^0_S$, we observed significant signals of χ_{c1} decays which are shown in Figure 2.

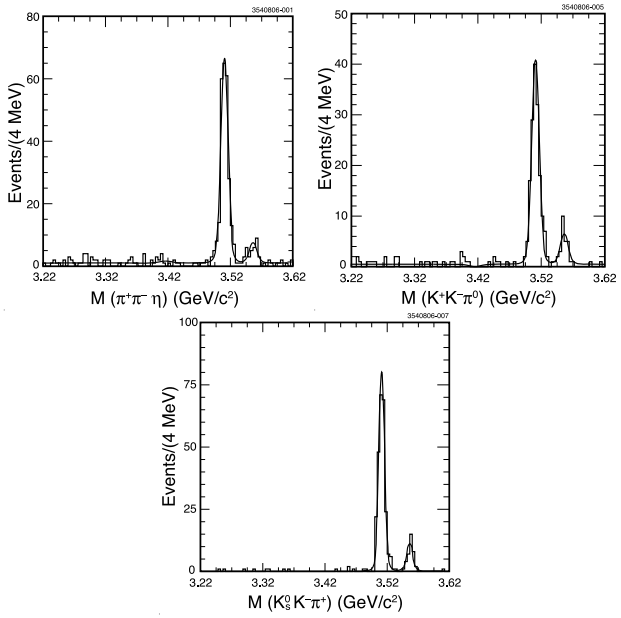

Figure 2: Invariant masses of $\pi^+\pi^-\eta$ (top-left), $K^+K^-\pi^0$ (top-right), and $K^0_SK^-\pi^+$ (bottom)

We performed Dalitz plot analyses based on these 3 modes in which we neglected any possible interference effects between resonances and polarization of χ_{c1}. We estimated there could be $\sim 20(15)\%$ variations in fit fractions for the $\pi\pi\eta$ ($KK\pi$) mode due to such a simplified model. Figure 3 shows the Dalitz plot for $\pi^+\pi^-\eta$ and Table II shows its resultant fit fractions for each source. It is interesting to note that our data demand a relatively large yield of a σ pole.

As for the $KK\pi$ mode, we performed simultaneous fits between $\chi_{c1} \to K^+K^-\pi^0$ and $\chi_{c1} \to K_SK\pi$ by taking advantage of isospin symmetry. Dalitz plots for these modes are shown in Figures 4 and 5. Table III shows their resultant fit fractions.

2.3. Four-body decay

We present a preliminary result on four-body decay of χ_{cJ} states in which we reconstructed $h^+h^-\pi^0\pi^0$, where $h = \pi$, K, p; $K^+K^-\eta\pi^0$; and $K^\pm\pi^\mp K^0_S\pi^0$. Results of this kind of study, many-body decays of

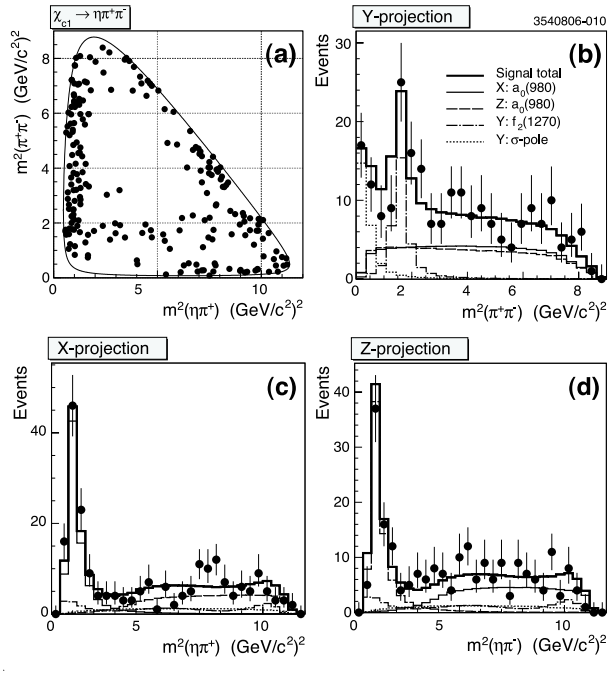

Figure 3: Dalitz plots for $\chi_{c1} \to \eta\pi^+\pi^-$.

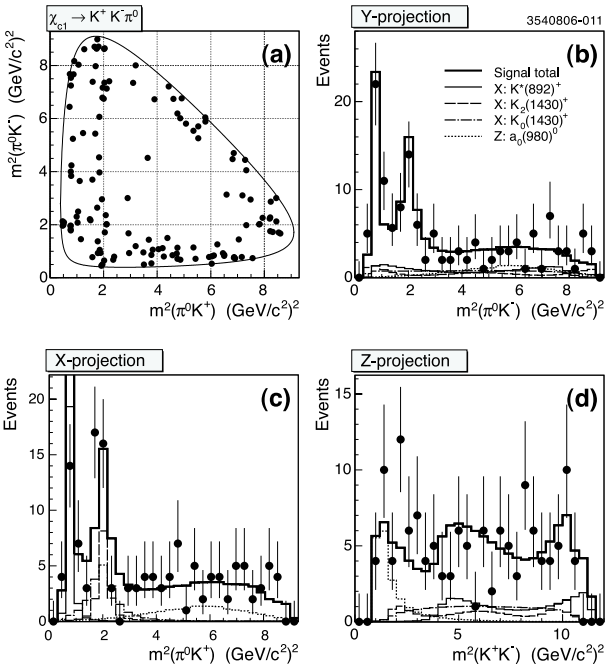

Figure 4: Dalitz plots for $\chi_{c1} \to K^+K^-\pi^0$.

χ_{cJ} states, should help to build a comprehensive understanding about the P-wave dynamics.

Clean signals were seen in all modes except $\chi_{c1} \to p\bar{p}\pi^0\pi^0$ for the first time as can be seen in Figure 6. Many resonant substructures were also seen for which we only considered significant ones ($\pi^+\pi^-\pi^0\pi^0$ and $K^\pm\pi^\mp K^0_S\pi^0$). The results are summarized in Table V.

Table I Branching fractions in units of 10^{-3}. Uncertainties are statistical, systematic due to detector effects plus analysis methods, and a separate systematic due to uncertainties in the $\psi(2S)$ branching fractions. Limits are at the 90% confidence level.

Mode	χ_{c0}	χ_{c1}	χ_{c2}
$\pi^+\pi^-\eta$	< 0.21	$5.0 \pm 0.3 \pm 0.4 \pm 0.3$	$0.49 \pm 0.12 \pm 0.05 \pm 0.03$
$K^+K^-\eta$	< 0.24	$0.34 \pm 0.10 \pm 0.03 \pm 0.02$	< 0.33
$p\bar{p}\eta$	$0.39 \pm 0.11 \pm 0.04 \pm 0.02$	< 0.16	$0.19 \pm 0.07 \pm 0.02 \pm 0.01$
$\pi^+\pi^-\eta'$	< 0.38	$2.4 \pm 0.4 \pm 0.2 \pm 0.2$	$0.51 \pm 0.18 \pm 0.05 \pm 0.03$
$K^+K^-\pi^0$	< 0.06	$1.95 \pm 0.16 \pm 0.18 \pm 0.14$	$0.31 \pm 0.07 \pm 0.03 \pm 0.02$
$p\bar{p}\pi^0$	$0.59 \pm 0.10 \pm 0.07 \pm 0.03$	$0.12 \pm 0.05 \pm 0.01 \pm 0.01$	$0.44 \pm 0.08 \pm 0.04 \pm 0.03$
$\pi^+K^-\overline{K}^0$	< 0.10	$8.1 \pm 0.6 \pm 0.6 \pm 0.5$	$1.3 \pm 0.2 \pm 0.1 \pm 0.1$
$K^+\bar{p}\Lambda$	$1.07 \pm 0.17 \pm 0.10 \pm 0.06$	$0.33 \pm 0.09 \pm 0.03 \pm 0.02$	$0.85 \pm 0.14 \pm 0.08 \pm 0.06$

Table II Fit results for $\chi_{c1} \to \eta\pi^+\pi^-$ Dalitz plot analysis. The uncertainties are statistical and systematic. Allowing for interference among the resonances changes the fit fractions by as much as 20% in absolute terms as discussed in the text.

Mode	Fit Fraction (%)
$a_0(980)^\pm\pi^\mp$	$75.1 \pm 3.5 \pm 4.3$
$f_2(1270)\eta$	$14.4 \pm 3.1 \pm 1.9$
$\sigma\eta$	$10.5 \pm 2.4 \pm 1.2$

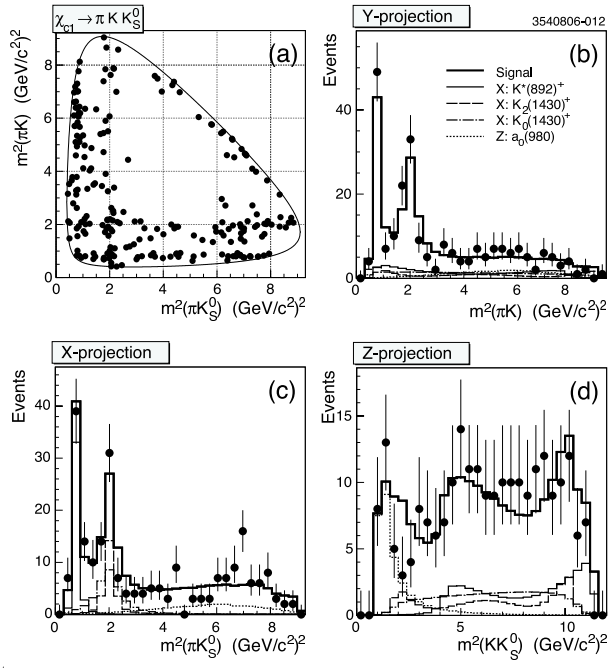

Figure 5: Dalitz plots for $\chi_{c1} \to \pi K K_S^0$.

The measured branching fraction of $\chi_{cJ} \to \rho^\pm\pi^\mp\pi^0$ is consistent with that of $\chi_{cJ} \to \rho^0\pi^+\pi^-$ as expected from isospin symmetry. Similar isospin symmetry is also seen in Table IV where the partial width

Table III Results of the combined fits to the $\chi_{c1} \to K^+K^-\pi^0$ and $\chi_{c1} \to \pi K K_S^0$ Dalitz plots. Allowing for interference among the resonances changes the fit fractions by as much as 15% in absolute terms as discussed in the text.

Mode	Fit Fraction (%)
$K^*(892)K$	$31.4 \pm 2.2 \pm 1.7$
$K_0^*(1430)K$	$30.4 \pm 3.5 \pm 3.7$
$K_2^*(1430)K$	$23.1 \pm 3.4 \pm 7.1$
$a_0(980)\pi$	$15.1 \pm 2.7 \pm 1.5$

of $\chi_c \to K^{*0}K^0\pi^0$ and that of $\chi_c \to K^{*\pm}K^\mp K^0$ are expected to be equal. Table IV also shows another good agreement with the isospin expectation of $\mathcal{B}(\chi_c \to K^{*0}K^0\pi^0)/\ \mathcal{B}(\chi_c \to K^{*0}K^\pm\pi^\mp) = 0.5$ and $\mathcal{B}(\chi_c \to K^{*0}K^0\pi^0)/\ \mathcal{B}(\chi_c \to K^{*\pm}\pi^\mp K^0) = 0.5$.

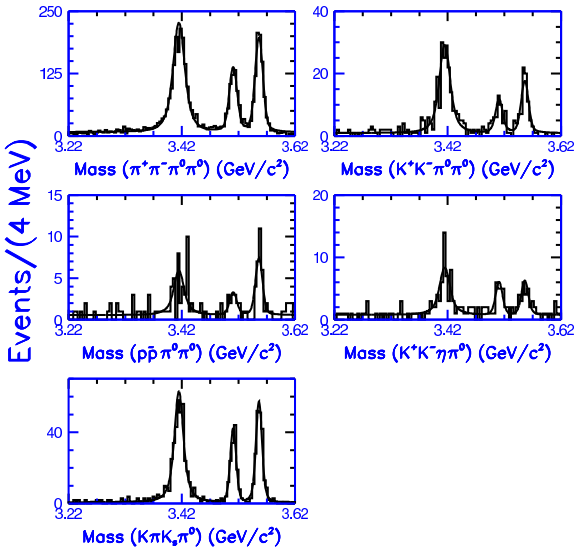

Figure 6: Preliminary result on 4-body decays of χ_{cJ}. Invariant masses of various combinations of hadrons are shown.

Table IV Branching fractions and combined error measurements for the isospin related $K^*K\pi$ intermediate modes are listed.

Mode	χ_{c0}	χ_{c1}	χ_{c2}
	B.F. (%)	B.F. (%)	B.F. (%)
$K^{*0}K^0\pi^0$	0.56±0.15	0.38±0.11	0.59±0.14
$K^{*0}K^\pm\pi^\mp$	-	-	0.90±0.25
$K^{*\pm}K^\mp\pi^0$	0.74±0.18	-	0.57±0.13
$K^{*\pm}\pi^\mp K^0$	0.96±0.25	-	0.90±0.25

3. Charmonium-like states above $D\bar{D}$

3.1. Y(4260)

Y(4260) was first discovered by the BaBar Collaboration via the reaction of $e^+e^- \to \gamma Y(4260) \to \gamma\pi^+\pi^- J/\psi$, $J/\psi \to \ell^+\ell^-$ [8]. Through the same production mechanism of initial state radiation, we also confirmed their observation based on data taken around the $\Upsilon(nS)$ resonances, where n is 1, 2, 3, and, 4 [9]. The invariant mass of $\pi^+\pi^- J/\psi$ based on such ISR production is shown in Figure 7.

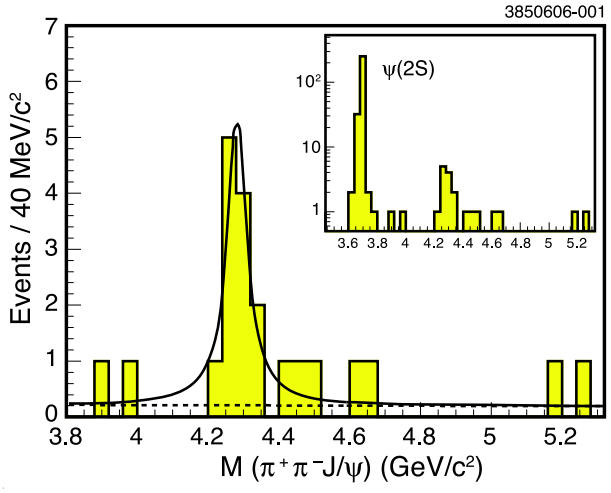

Figure 7: Distribution of invariant mass of $\pi^+\pi^- J/\psi$ produced in ISR.

We further confirmed BaBar's observation in data taken directly at $\sqrt{s}$ = 4260 MeV [10] at 11 σ significance. We also observed $Y(4260) \to \pi^0\pi^0 J/\psi$ for the first time at significance of 5.1 σ and had the first evidence for $Y(4260) \to K^+K^- J/\psi$ (3.7σ). We measured e^+e^- cross sections as $\sigma(\pi^+\pi^- J/\psi) = (58^{+12}_{-10} \pm 4)$ pb, $\sigma(\pi^0\pi^0 J/\psi) = (23^{+12}_{-8} \pm 1)$ pb, and $\sigma(K^+K^- J/\psi) = (9^{+9}_{-5} \pm 1)$ pb. Using scan data taken between $\sqrt{s}$ of 3970 MeV and 4260 MeV, we also searched in 12 additional modes (transitions down to $\psi(2S)$, χ_{cJ}, and J/ψ). No evidence of strong signals were seen for which we set upper limits at 90% confidence level. The results are summarized in Table VI.

The observation of $Y(4260) \to \pi^0\pi^0 J/\psi$ is inconsistent with the $\chi_{cJ}\rho^0$ molecular model [11]. Our observation of $\pi^0\pi^0 J/\psi$ rate being about half of $\pi^+\pi^- J/\psi$ rate disagrees with the prediction of the baryonium model [12]. Evidence for the $K^+K^- J/\psi$ signal is not compatible with these two models either. Table VI also shows that Y(4160) behaves very differently compared to other charmonium states above $D\bar{D}$ threshold such as $\psi(4040)$ and $\psi(4160)$ for which we set upper limits in terms of cross section ($\sigma(e^+e^- \to X)$) and branching fractions.

3.2. X(3872) and Mass of neutral D meson

Since X(3872) was discovered by Belle Collaboration [13] and subsequently confirmed by other experiments ([14],[15],[16]), many theoretical models have been proposed. Perhaps the most provocative theoretical suggestion is that X(3872) is a loosely bound state of D^0 and $\bar{D}^{*0}$ mesons [17]. This idea arises mainly because $M(D^0) + M(D^{*0}) - M(X(3872))$ is very small. Using the average value of $M(D^0)$ of 2006 Particle Data Group [1], 1864.1 ± 1.0 MeV, we have -0.9 ± 2.1 MeV for the above difference or for the binding energy if we assume it is a bound state of D^0 and $\bar{D}^{*0}$ mesons. The large uncertainty in the difference is partially due to the rather large uncertainty in mass of D^0 meson. This was the motivation to measure $M(D^0)$ more precisely using our 281 pb^{-1} of data taken at $\psi(3770)$.

We used a clean (charged particles only) mode of D meson decay, $D^0 \to K_S\phi$ where $K_S \to \pi^+\pi^-$ and $\phi \to K^+K^-$. Invariant masses of $\pi^+\pi^-$ and K^+K^- are shown in Figures 8 and 9 respectively. Figure 10 shows the invariant mass of $K_SK^+K^-$ from which we obtained $M(D^0) = 1864.847 \pm 0.150 \pm 0.095$ MeV [18]. We then have $M(D^0)+M(D^{*0})-M(X(3872)) = +0.6 \pm 0.6$ MeV. This provides a strong constraint for the theoretical predictions for the decays of X(3872) if it is a bound state of D^0 and $\bar{D}^{*0}$ mesons. The uncertainty in its binding energy is now calling for more precise measurement on mass of X(3872) itself.

4. Properties of η

It has been almost half a century since the η meson was discovered [19]. Since then, many measurements have been made by many experiments. Still, almost all exclusive branching fractions are determined as *relatives* to other η decays.

Based on the 27M $\psi(2S)$ sample, we measured almost all the major modes (99% of generic decays of η) which allowed us to determine the major branching fractions [20]. We obtained the η sample through

Table V Branching fractions (B.F.) with statistical and systematic uncertainties are shown. The symbol "×" indicates product of B.F.'s. The third error in each case is due to the $\psi(2S) \to \gamma\chi_c$ branching fractions. Upper limits shown are at 90% C.L and include all the systematic errors. The measurements of the three-hadron final states are inclusive branching fractions, and do not represent the amplitudes for the three-body non-resonant decays.

Mode	χ_{c0}	χ_{c1}	χ_{c2}
	B.F.(%)	B.F.(%)	B.F.(%)
$\pi^+\pi^-\pi^0\pi^0$	3.54±0.10±0.43±0.18	1.28±0.06±0.16±0.08	1.87±0.07±0.23±0.13
$\rho^+\pi^-\pi^0$	1.48±0.13±0.18±0.08	0.78±0.09±0.09±0.05	1.12±0.08±0.14±0.08
$\rho^-\pi^+\pi^0$	1.56±0.13±0.19±0.08	0.78±0.09±0.09±0.05	1.11±0.09±0.13±0.08
$K^+K^-\pi^0\pi^0$	0.59±0.05±0.08±0.03	0.12±0.02±0.02±0.01	0.21±0.03±0.03±0.01
$p\bar{p}\pi^0\pi^0$	0.11±0.02±0.02±0.01	< 0.05	0.08±0.02±0.01±0.01
$K^+K^-\eta\pi^0$	0.32±0.05±0.05±0.02	0.12±0.03±0.02±0.01	0.13±0.04±0.02±0.01
$K^\pm\pi^\mp K^0\pi^0$	2.64±0.15±0.31±0.14	0.92±0.09±0.11±0.06	1.41±0.10±0.16±0.10
$K^{*0}K^0\pi^0 \times K^{*0} \to K^\pm\pi^\mp$	0.37±0.09±0.04±0.02	0.25±0.06±0.03±0.02	0.39±0.07±0.05±0.03
$K^{*0}K^\pm\pi^\mp \times K^{*0} \to K^0\pi^0$			0.30±0.07±0.04±0.02
$K^{*\pm}K^\mp\pi^0 \times K^{*\pm} \to \pi^\pm K^0$	0.49±0.10±0.06±0.03		0.38±0.07±0.04±0.03
$K^{*\pm}\pi^\mp K^0 \times K^{*\pm} \to K^\pm\pi^0$	0.32±0.07±0.04±0.02		0.30±0.07±0.04±0.02
$\rho^\pm K^\mp K^0$	1.28±0.16±0.15±0.07	0.54±0.11±0.06±0.03	0.42±0.11±0.05±0.03

Table VI For each mode $e^+e^- \to X$, for three center-of-mass regions: the detection efficiency, ϵ; the number of signal [background] events in data, $N_{\rm s}$ [$N_{\rm b}$]; the cross-section $\sigma(e^+e^- \to X)$; and the branching fraction of $\psi(4040)$ or $\psi(4160)$ to X, $\mathcal{B}$. Upper limits are at 90% CL. '–' indicates that the channel is kinematically or experimentally inaccessible.

Channel	$\sqrt{s} = 3970 - 4060$ MeV					$\sqrt{s} = 4120 - 4200$ MeV					$\sqrt{s} = 4260$ MeV			
	ϵ (%)	$N_{\rm s}$	$N_{\rm b}$	σ (pb)	$\mathcal{B}$ (10^{-3})	ϵ (%)	$N_{\rm s}$	$N_{\rm b}$	σ (pb)	$\mathcal{B}$ (10^{-3})	ϵ (%)	$N_{\rm s}$	$N_{\rm b}$	σ (pb)
$\pi^+\pi^- J/\psi$	37	12	3.7	$9^{+5}_{-4}\pm2$	< 4	38	13	3.7	$8^{+4}_{-3}\pm2$	< 4	38	37	2.4	$58^{+12}_{-10}\pm4$
$\pi^0\pi^0 J/\psi$	20	1	1.9	< 8	< 2	21	5	0.9	$6^{+5}_{-3}\pm1$	< 3	22	8	0.3	$23^{+12}_{-8}\pm1$
$K^+K^- J/\psi$			–			7	1	0.07	< 20	< 5	21	3	0.07	$9^{+9}_{-5}\pm1$
$\eta J/\psi$	19	12	9.5	< 29	< 7	16	15	8.8	< 34	< 8	16	5	2.7	< 32
$\pi^0 J/\psi$	23	2		< 10	< 2	22	1		< 6	< 1	22	1		< 12
$\eta' J/\psi$			–			11	4	2.5	< 23	< 5	11	0	1.5	< 19
$\pi^+\pi^-\pi^0 J/\psi$	21	1		< 8	< 2	21	0		< 4	< 1	22	0		< 7
$\eta\eta J/\psi$			–					–			6	1		< 44
$\pi^+\pi^-\psi(2S)$			–			12	0		< 15	< 4	19	0		< 20
$\eta\psi(2S)$			–					–			15	0		< 25
$\omega\chi_{c0}$			–					–			9	11	11.5	< 234
$\gamma\chi_{c1}$	26	9	8.1	< 50	< 11	26	11	8.7	< 45	< 10	26	1	3.3	< 30
$\gamma\chi_{c2}$	25	6	8.0	< 76	< 17	26	10	8.6	< 79	< 18	27	4	3.3	< 90
$\pi^+\pi^-\pi^0\chi_{c1}$	6	0		< 47	< 11	8	0		< 26	< 6	9	0		< 46
$\pi^+\pi^-\pi^0\chi_{c2}$	4	0		< 141	< 32	8	0		< 56	< 13	9	0		< 96
$\pi^+\pi^-\phi$	17	26	3.0	< 12	< 3	17	17	6.0	< 5	< 1	18	7	5.5	< 5

a two-body decay of $\psi(2S)$, $\psi(2S) \to \eta J/\psi$ where J/ψ subsequently decays to two leptons (e^+e^- or $\mu^+\mu^-$). That is, we have sample of about 0.1M η decays with a di-lepton tag on J/ψ.

We first constrained the invariant mass of di-leptons to be the known mass of J/ψ. We then combined the fitted J/ψ with η decay products and constrained further to be the mass of $\psi(2S)$. In this analysis, the η decay modes we considered were $\eta \to \gamma\gamma$, $3\pi^0$, $\pi^+\pi^-\pi^0$, $\pi^+\pi^-\gamma$ and $e^+e^-\gamma$. According to Ref. [1], the sum of these 5 rates amounts to 99.88% of the total η decays. We then took ratios between efficiency-corrected yields separately for each of $J/\psi \to e^+e^-$ and $\mu^+\mu^-$ cases in which all lepton related systematic

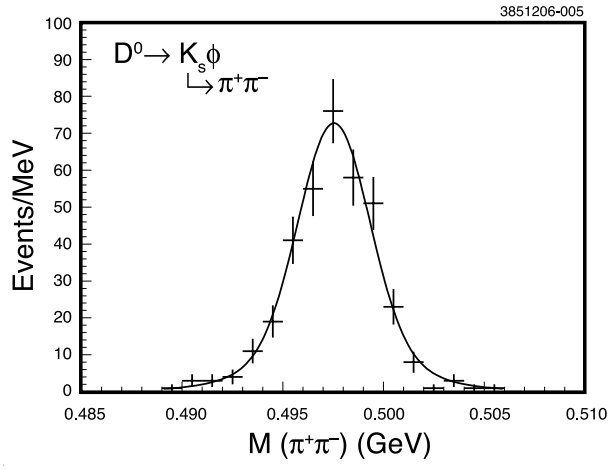

Figure 8: Invariant mass of $\pi^+\pi^-$.

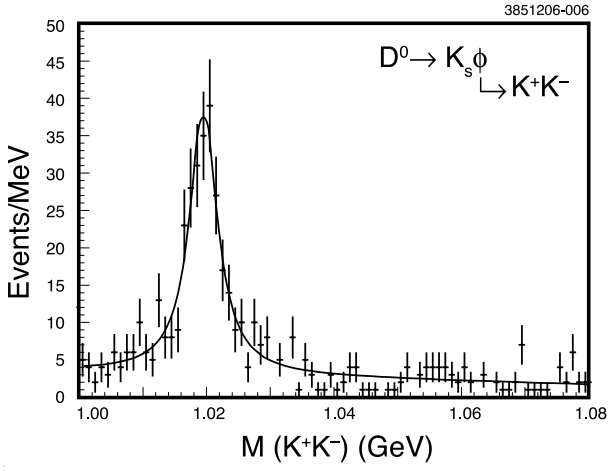

Figure 9: Invariant mass of K^+K^-.

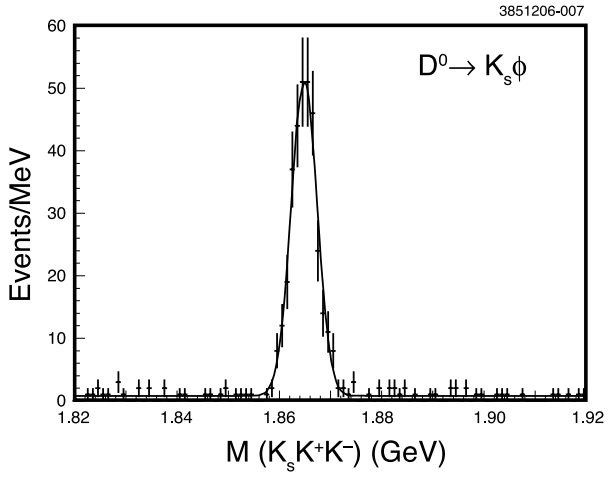

Figure 10: Invariant mass of $K_S K^+ K^-$.

Table VII Ratios of η branching fractions. For each combination, the efficiency ratio, separately for $J/\psi \to e^+e^-$ and $J/\psi \to \mu^+\mu^-$, the level of consistency between the $J/\psi \to e^+e^-$ and $\mu^+\mu^-$ result, expressed in units of Gaussian standard deviations, $\sigma_{\mu\mu/ee}$, and the combined result for the branching ratio. The dagger symbol indicates that this result is most precise measurement to date.

Channel	eff. ratio		$\sigma_{\mu\mu/ee}$	branching fraction ratio
	$\mu\mu$	ee		
$3\pi^0/\gamma\gamma$	0.15	0.15	1.0	$0.884 \pm 0.022 \pm 0.019$
$pi^+\pi^-\pi^0/\gamma\gamma$	0.50	0.49	−2.2	$0.587 \pm 0.011 \pm 0.009^\dagger$
$\pi^+\pi^-\gamma/\gamma\gamma$	0.63	0.60	0.2	$0.103 \pm 0.004 \pm 0.004^\dagger$
$e^+e^-\gamma/\gamma\gamma$	0.53	0.52	0.1	$0.024 \pm 0.002 \pm 0.001^\dagger$
$3\pi^0/\pi^+\pi^-\pi^0$	0.30	0.32	2.1	$1.496 \pm 0.043 \pm 0.035^\dagger$
$\pi^+\pi^-\gamma/\pi^+\pi^-\pi^0$	1.27	1.24	1.1	$0.175 \pm 0.007 \pm 0.006$
$e^+e^-\gamma/\pi^+\pi^-\pi^0$	1.07	1.06	0.5	$0.041 \pm 0.003 \pm 0.002^\dagger$
$e^+e^-\gamma/\pi^+\pi^-\gamma$	0.84	0.86	0.0	$0.237 \pm 0.021 \pm 0.015$

uncertainties were canceled. The resulting ratios of η branching fractions are summarized in Table VII.

Figure 11 shows a graphical version of comparison in terms of ratios of branching fractions to the single most precise other measurements (top of Figure 11).

By assuming that the 5 exclusive channels we considered in this analysis cover the all η decay modes, we were also able to extract absolute branching fractions of these 5 modes. Other possible η decay modes are either now allowed and/or found to be less than 0.2% of generic decays η [1]. We included 0.3% as a possible systematic uncertainty in the absolute branching fraction measurements. The results are summarized in Table VIII and also shown graphically in Figure 11 in terms of ratio of our branching fractions to the PDG 2006 global fit (bottom of Figure 11). Several of the relative and absolute branching fractions obtained in this analysis are either the most precise to date or first measurements.

Further more, we also measured the mass of η meson [22]. This was motivated by two recent precision measurements that were inconsistent with each other. In 2002, the NA48 Collaboration reported $M_\eta = 547.843 \pm 0.030 \pm 0.041$ MeV [23], while in 2005, GEM Collaboration reported $M_\eta = 547.311 \pm 0.028 \pm 0.032$ MeV [24] which was 8 standard deviations below NA48's result.

We used the same η sample described previously in this Section but used only 4 decay modes, $\eta \to \gamma\gamma$, $3\pi^0$, $\pi^+\pi^-\pi^0$, and $\pi^+\pi^-\gamma$ while, again, constraining masses of J/ψ and $\psi(2S)$. Our result, the average of the 4 η decay modes, is $M_\eta = 547.785 \pm 0.017 \pm 0.057$ MeV which has comparable precision to both NA48 and GEM results, but is consistent with the former and 6.5 standard deviations larger than the later. We note that the KLOE Collaboration also recently measured mass of the η meson to be $547.873 \pm 0.007 \pm 0.031$ MeV which was presented at the 2007 Lepton-Photon conference [25].

Table VIII For each η decay channel, absolute branching fraction measurements for $J/\psi \to e^+e^-$ and $J/\psi \to \mu^+\mu^-$ combined, with statistical and systematic uncertainties (middle column), as determined in this work. The last column shows the PDG fit result [1]. All but $\gamma\gamma$ are first measurements.

Channel	this work (%)	PDG [1] (%)
$\gamma\gamma$	$38.45 \pm 0.40 \pm 0.36$	39.38 ± 0.26
$3\pi^0$	$34.03 \pm 0.56 \pm 0.49$	32.51 ± 0.28
$\pi^+\pi^-\pi^0$	$22.60 \pm 0.35 \pm 0.29$	22.7 ± 0.4
$\pi^+\pi^-\gamma$	$3.96 \pm 0.14 \pm 0.14$	4.69 ± 0.11
$e^+e^-\gamma$	$0.94 \pm 0.07 \pm 0.05$	0.60 ± 0.08

5. Summary

I have presented confirmation of BaBar's observation of Y(4260) in di-pion transition to J/ψ along with a new observation through neutral di-pion transition. Our precision measurement on $M(D^0)$ calls for more precise measurement on $M(X(3872))$. With 3M $\psi(2S)$ sample, we have results on two-, three-, and four-body decays of χ_{cJ} states in which many substructures were seen in three- and four-body modes. Dalitz plot analyses were done for the case of 3-body decays. More detailed analyses can be done with the full 27M $\psi(2S)$ sample. Using the 27M sample, we performed precision measurements on $\mathcal{B}(\eta \to X)$ and $M(\eta)$.

References

[1] W. M. Yao *et al.* [Particle Data Group], J. Phys. G **33**, 1 (2006).

[2] G. S. Adams *et al.* (CLEO Collaboration), Phys. Rev. D **75**, 071101(R) (2007).

[3] J. Bai *et al.* (BES Collaboration), Phys. Rev. D **67**, 032004 (2003).

[4] M. Andreotti *et al.* (E-835 Collaboration), Phys. Rev. D **72**, 112002 (2005).

[5] Q. Zhao, Phys. Rev. D **72**, 074001 (2005).

[6] S. Athar *et al.* (CLEO Collaboration), Phys. Rev. D **75**, 032002 (2007).

[7] M. Ablikim *et al.* (BES Collaboration), Phys. Rev. D **74**, 072001 (2006).

[8] B. Aubert *et al.* (*BaBar* Collaboration), Phys. Rev. Lett. **95**, 142001 (2005).

[9] Q. He *et al.* (CLEO Collaboration), Phys. Rev. D **74**, 091104 (2006).

[10] T. E. Coan *et al.* (CLEO Collaboration), Phys. Rev. Lett. **96**, 162003 (2006).

[11] X. Liu, X.-Q. Zeng, and X.-Q. Li, Phys. Rev. D **72**, 054023 (2005).

[12] C.-F. Qiao, he-ph/0510228 (2005).

[13] S. K. Choi *et al.* (Belle Collaboration), Phys. Rev. Lett. **91**, 262001 (2003).

[14] D. Acosta *et al.* (CDF II Collaboration), Phys. Rev. Lett. **93**, 072001 (2004).

[15] V. M. Abazov *et al.* (DØ Collaboration), Phys. Rev. Lett. **93**, 162002 (2004).

[16] B. Aubert *et al.* (*BaBar* Collaboration), Phys. Rev. D **71**, 071103 (2005).

[17] E. S. Sanson, Phys. Lett. **B588**, 189 (2004); N. A. Törnqvist, Phys. Lett. **B599**, 209 (2004); M. B. Voloshin, Phys. Lett. **B579**, 316 (2004).

[18] C. Cawlfield *et al.* (CLEO Collaboration), Phys. Rev. Lett. **98**, 092002 (2007).

[19] A. Pevsner *et al.*, Phys. Rev. Lett. **7**, 421 (1961).

[20] A. Lopez *et al.* (CLEO Collaboration), Phys. Rev. Lett. **99**, 122001 (2007).

[21] M. Ablikim *et al.* (BES Collaboration), Phys. Rev. D **73**, 052008 (2006); D. Alde *et al.*, Z. Phys. **C25**, 225 (1984); Yad. Fiz. **40**, 1447 (1984); R. R. Akhmetshin *et al.* (CMD-2 Collaboration), Phys. Lett. **B509**, 217 (2001); J. J. Thaler *et al.*, Phys. Rev. D **7**, 2569 (1973).

[22] D. H. Miller *et al.* (CLEO Collaboration), Phys. Rev. Lett. **99**, 122002 (2007).

[23] A. Lai *et al.* (NA48 Collaboration), Phys. Lett. **B533**, 196 (2002).

[24] M. Abdel-Bary *et al.* (GEM Collaboration), Phys. Lett. **B619**, 281 (2005).

[25] F. Ambrosino *et al.* (KLOE Collaboration), arXiv:0707.4616 (contributed paper to Lepton Photon 2007).

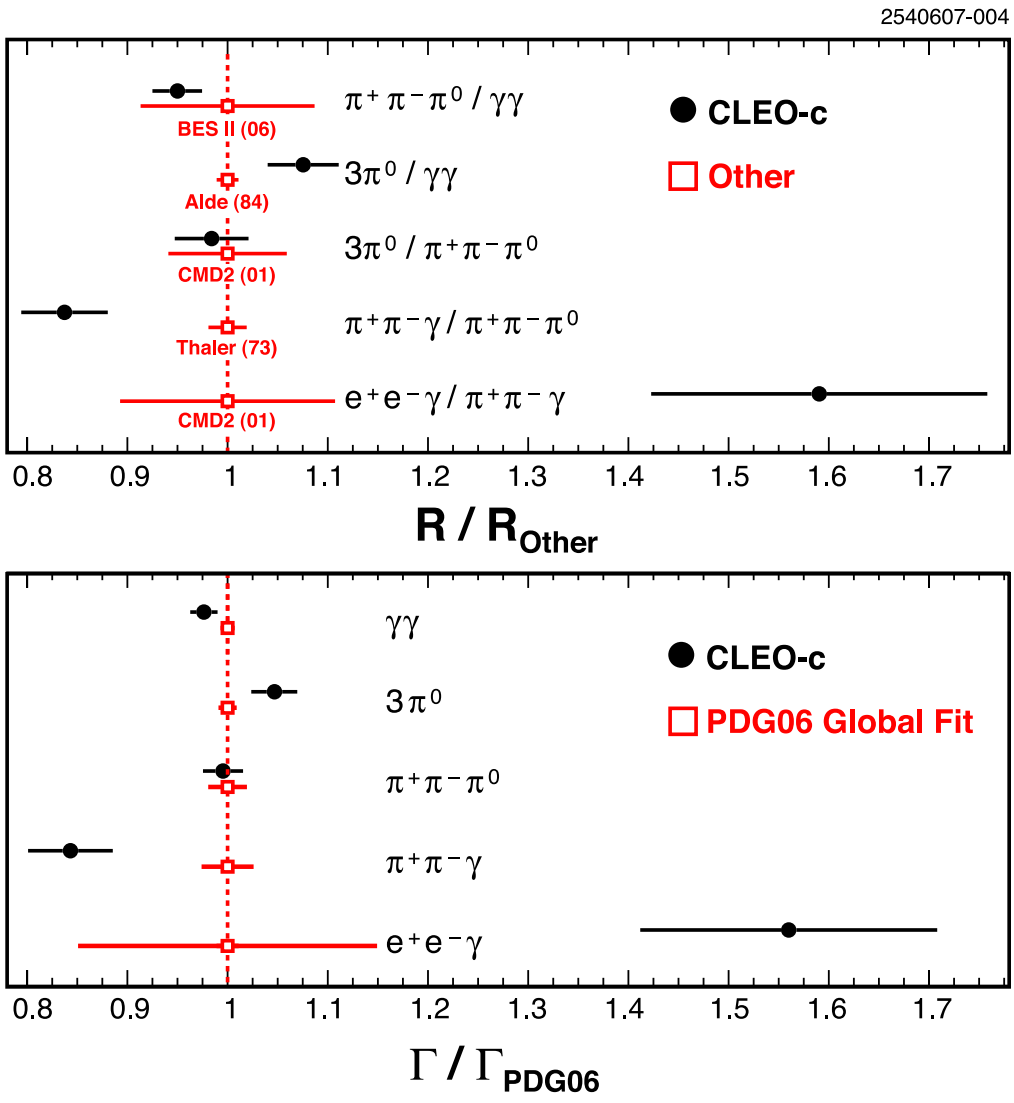

Figure 11: Comparison of the results obtained in this analysis with the most precise measurements from other experiments [1],[21] (top), and the PDG 2006 global fits [1] (bottom).